Level densities of ^{28}Al, ^{29}Si, and ^{41}Ca inferred from fluctuation measurements

W. Abfalterer, R. W. Finlay, S. M. Grimes, and V. Mishra*
Ohio University, Athens, Ohio 45701
(Received 19 October 1992)

Neutron total cross sections for ^{27}Al, ^{28}Si, and ^{40}Ca have been measured with good statistics ($\sim 1\%$) and good energy resolution over the energy range $4 \leq E_n \leq 20$ MeV. Two techniques have been used to infer the level density of the compound nuclei. The first is the conventional procedure of deducing an average level width and relating this to the level density. An alternative method is to deduce the level density from the magnitude of the variance of the cross section. A previous study of these two techniques suggested that the two yielded results which were not completely consistent. Our examination of the discrepancies indicates that they are reduced but not eliminated with better data. It seems likely that a part of the problem is the uncertainty in input parameters.

PACS number(s): 21.10.Ma, 24.60.Ky

I. INTRODUCTION

Fluctuation measurements have been used extensively to study level densities in the continuum ($E \gtrsim 12$ MeV) [1–3]. Even when the energy is high enough that levels in the compound nucleus overlap, it can be shown [1] that cross sections for compound nuclear processes will show variations with energy on a scale consistent with the average level width. Either cross sections to particular final states or total cross sections may be used for this analysis. An interesting result of the theory of fluctuations is that two separate techniques exist for inferring the compound nuclear level density from the fluctuation behavior. The first involves determining the average level width Γ and then relating this to the level density in the compound nucleus through the expressions

$$T_i^J = 2\pi\Gamma_i / D_J \ , \tag{1}$$

$$\Gamma = \sum_i \Gamma_i \ , \tag{2}$$

where i denotes a particular decay channel, Γ_i is the decay width to that channel, D_J is the level spacing in the compound nucleus with spin J, and T_i^J is the transmission coefficient for the ith channel coupled to spin J. As can be seen, this approach relates the D value (inverse of the compound level density) to sums of transmission coefficients over decay channels and to the average level width.

A second approach is to study the variance of the cross section. It has been shown that

$$\mathrm{var}\sigma_T = \left\{ \frac{\pi\lambda^2}{(2i+1)(2I+1)} \right\}^2 \frac{1}{\pi\Gamma\omega(E)} \times \sum_J \frac{(2J+1)^2}{H(J)} \sum_l (T_{nl}^J)^2 \ , \tag{3}$$

where σ_T is the total neutron cross section for a particular target, λ is the reduced wavelength of the neutron, J is the spin of the compound nucleus, and i and I are the spins of the projectile and target, respectively. T is the transmission coefficient, and the compound level density is $\rho(E,J) = H(J)\omega(E)$. Note that this method, in fact, requires both Γ and the variance, but does not need the level densities in the residual nuclei. Virtually all of the fluctuation measurements reported have based level density determinations on method 1 (the gamma method), but a few analyses [4,5] have utilized method 2 (the variance technique). To our knowledge, only Ref. [6] has compared the two procedures. The results were not completely consistent, and Mishra *et al.* [6] considered a number of possible explanations for the discrepancies. In addition to difficulties with assumptions in the analysis, a possible explanation could be the limitations imposed by the quality of the data. Although the resolution of the measurements of Mishra *et al.* was superior to previous measurements, the statistical accuracy was only 2–3 %, which limited the reliability of the comparison.

The present measurements were undertaken as part of a program to measure total neutron cross sections for a number of targets at energies between 5 and 600 MeV. These data [7,8] were acquired at the WNR facility at Los Alamos National Laboratory and were intended to give additional information about optical model potentials above 50 MeV. The quality of the data was such that for some targets the measurements yielded measurements of better quality than were previously available in the region below 20 MeV as well.

II. EXPERIMENTAL TECHNIQUES

The neutron total cross section is determined by measuring the attenuation in a neutron beam produced by a known amount of material. If N_0 is the number of counts without a sample and N_1 is the number with a sample, then

*Present address: Washington University, School of Medicine, St. Louis, MO 63110.

$$\sigma=\frac{1}{nL}\ln\frac{N_0}{N_1} ,$$

where n is the number of nuclei per unit volume and L is the length of the sample.

Neutrons were provided by the white source at WNR (Los Alamos). A beam of 800-MeV protons impinges on a W target and produces neutrons over the range from kilovolts to nearly 800 MeV. The time width of the beam is less than 1 ns, allowing the identification of neutron energies from time of flight.

Open beam and target spectra γ peaks were shifted to coincide. The analytic dead time correction [9] takes into account that low-energy neutrons have a smaller probability of being counted than high-energy neutrons. It also corrects for variations of the beam intensity. Typical correction factors applied to the observed number of counts were as high as 1.7. Inclusion of beam intensity variation altered factors by less than 0.1%.

While events were being processed by the data acquisition system, no other events could be accepted. By knowing the total number of beam pulses and the number of times the system was alive, the true spectra are obtained by multiplication with the ratio of these numbers. Typical factors ranged between 1.1 and 1.8. The number of live beam pulses was corrected for the number of veto counts.

The spectra were normalized to the monitor counts, and the time-independent background was subtracted. Using the two-sample technique [10], the time-dependent background was determined and found negligible. Corrections because of inscattering and beam hardening were found inconsequential.

The energy resolution was found to be better than 3 and 19 keV at 4 and 18 MeV neutron energy, respectively. Accuracy due to counting statistics is better than 1% for ^{27}Al and ^{28}Si and better than 2% for ^{40}Ca. Unlike the previous reports on this experiment [7,8] in which the data were averaged over 1% energy bins for spherical optical model analysis, the present study utilizes the full energy resolution of the original experiment.

A plot of the data for the lowest-energy region for ^{27}Al is shown in Fig. 1. Also shown for comparison are the data points of Carlson and Barschall [4]. Good agreement in the structure and magnitude of the cross section is seen, with somewhat sharper structure found in the present data.

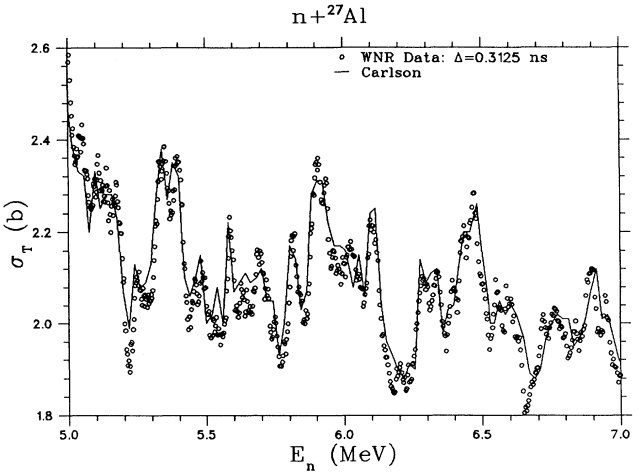

FIG. 1. Comparison of the present total cross section data on ^{27}Al with the data of Carlson and Barschall [4] in the energy range 5 MeV $\leq E_n \leq 7$ MeV. The better resolution of the present data causes sharper peaks and valleys in the energy dependence, but good agreement in energy scale and average magnitude can be seen.

III. ANALYSIS

Determination of the average level width can be made in three different ways. Originally, widths were determined by calculating the autocorrelation function

$$F(\epsilon)=\langle[\sigma(E+\epsilon)-\langle\sigma\rangle][\sigma(E)-\langle\sigma\rangle]\rangle$$

$$=\frac{F(0)}{1+(\epsilon/\Gamma)^2} ,$$

where $F(0)$ is the variance of the cross section. By calculating this expression for various values of ϵ, that value for which $F(\epsilon)=\frac{1}{2}F(0)$ can be found. Subsequently, it was proposed that the number of maxima, N, per unit energy be counted; the value of Γ would then be [11]

$$\Gamma=0.55/N . \quad (4)$$

Finally, the cross section can be expanded in a Fourier series in the form

$$\sigma(E)=\sum_{K=0}^{m} a_K\cos\frac{2\pi KE}{\Delta}+\sum_{K'=1}^{m} b_{K'}\sin\frac{2\pi K'E}{\Delta} ,$$

where m will be Δ/d, where Δ is the energy interval to be expanded and d is the spacing between points, and a_K and b_K are the usual Fourier expansion coefficients. It has been shown that the quantity S_K defined as

$$S_K=a_K^2+b_K^2=4\pi\frac{\Gamma}{\Delta}(\mathrm{var}\sigma)e^{-2\pi K\Gamma/\Delta} , \quad (5)$$

providing a method for determining Γ.

Richter [3] concludes that of these three methods there is a slight preference for the Fourier series method. All of the three can be adversely affected by poor resolution or poor statistics, but for good data, Richter [3] finds somewhat smaller errors due to the finite range of data with the Fourier series method. Statistical errors cause a "white noise" contribution to the spectrum; this effectively adds a constant to each S_K, and so a fit is usually made with a constant term added to the right-hand side of Eq. (5). Finally, modulations in the energy dependence of the cross section due to optical model effects or long-range changes in cross section can affect Γ as well; these can be dealt with by discarding the lowest-order S_K values and fitting only the values beyond a certain S_K, since variations over large energy ranges are seen in low-order K values.

Similarly, the variance is also affected by long-range energy modulations. Instead of calculating the variance directly, the value was calculated from the constant mul-

tiplier in Eq. (5), since once Γ is determined all other quantities are known. In fact, since the variance method depends on the product of the variance and width, errors in Γ will not necessarily be compounded in using the variance method, given the appearance of the product $\Gamma \mathrm{var}\sigma$ in the constant to be fitted. A typical fit is shown in Fig. 2.

Figures 3–5 show the level densities inferred for ^{28}Al, ^{29}Si, and ^{41}Ca from fluctuations. The combination of data with good resolution and statistical accuracy and the large energy range yields a number of values for the level density.

To provide a comparison between the gamma and variance methods, the level density values were calculated using both techniques. For the variance method, the only additional input parameters needed are transmission coefficients for neutrons incident on the target and the spin cutoff parameter, which is needed to specify $H(J)$. Optical potential parameters of Rapaport, Kulkarni, and Finlay [12] were used to calculate transmission coefficients for neutrons, and those of Becchetti and Greenlees [13] and McFadden and Satchler [14] were used for protons and alpha particles, respectively, while the single-particle energies proposed by Seeger and Perisho [15] and Seeger and Howard [16] were used to calculate the spin cutoff parameters using a microscopic Fermi gas code [17]. Relatively small uncertainty exists in the spin cutoff parameter ($< 10\%$) based on the comparison between the two single-particle sets, and small differences are also seen if the neutron transmission coefficients are evaluated with the potential of Becchetti and Greenlees [13] instead of that of Rapaport, Kulkarni, and Finlay [12]. Other uncertainties could come from the fact that the derivation of Eq. (3) assumes that the total level width is independent of J, which allows Γ to be factored out of the sum. If this assumption is relaxed, the sum can be evaluated using the relative J dependence predicted by a Hauser-Feshbach calculation. Less than 10% changes resulted from this alternative calculation. Other uncertainties result from the determination of the product $\Gamma \mathrm{var}\sigma$. As was previously discussed, this was done using the procedure of Mishra *et al.* [6]. Fits to the S_K values from a Fourier series expansion were calculated for various minimum values of K. Eliminating the first few values produced successively smaller values of χ^2 for the fit of Eq. (5) to the data. As the point where the χ^2 stabilized was reached, it was found that the value of Γ, which to this point dropped as each term was deleted, also stabilized. This value of Γ was selected, and the value of $\Gamma \mathrm{var}\sigma$ obtained with this minimum K was used to deduce the level density. Note that this value of $\mathrm{var}\sigma$ is not the one which would be calculated directly from the data, but is modified because of the deletion of long-range modulation effects.

Evaluation of the level density from the gamma values is carried out with the same approach as by Mishra *et al.*

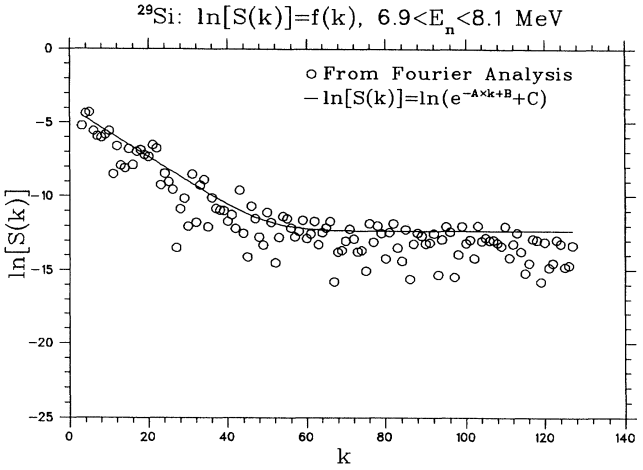

FIG. 2. Plots of the S_k values for the total cross section data for silicon for energies in the range 6.9 MeV $\leq E_n \leq 8.1$ MeV. The solid line shows a fit of the form exponential plus constant to the S_k distribution.

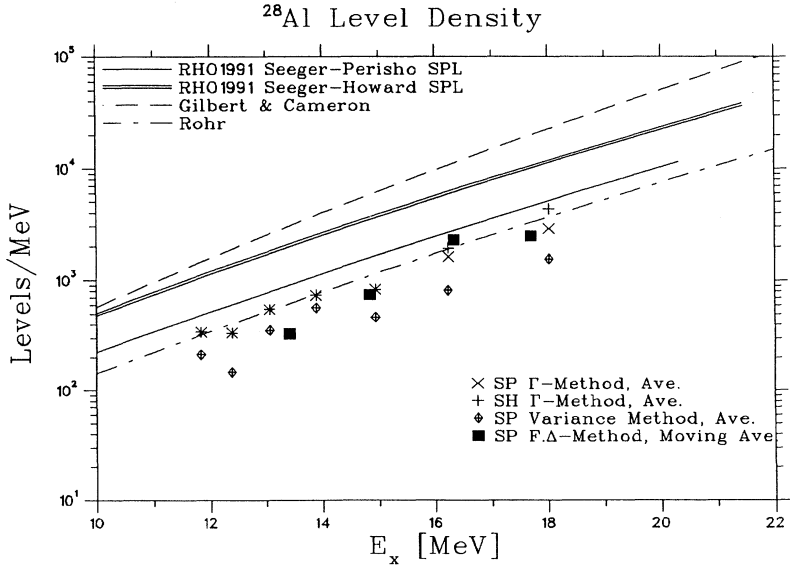

FIG. 3. Level density of ^{28}Al inferred from fluctuation measurements compared with calculations and predictions. The × and + marks denote values derived from the gamma method with level densities in the final nuclei given by microscopic predictions based on Seeger-Perisho [15] and Seeger-Howard [16] single-particle states, respectively. The ◇ symbols denote values obtained from the variance method, and the □ symbols those derived from the nonoverlapping level formalism. Solid and double solid lines denote the microscopic calculation with Seeger-Perisho and Seeger-Howard levels, respectively, and the dashed and dot-dashed curves show the predictions of Gilbert and Cameron [20] and Rohr [19], respectively.

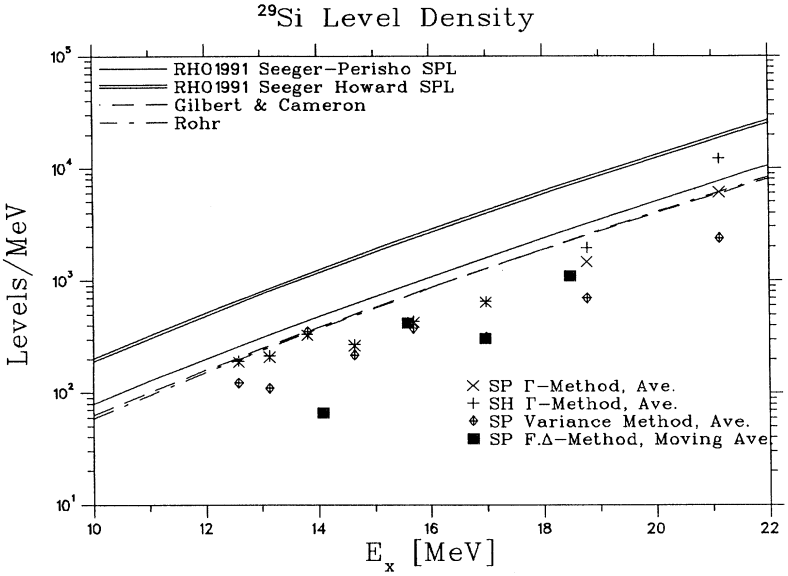

FIG. 4. Level density of ^{29}Si inferred from fluctuation measurements compared with calculations and predictions. The × and + marks denote values derived from the gamma method with level densities in the final nuclei given by microscopic predictions based on Seeger-Perisho [15] and Seeger-Howard [16] single-particle states, respectively. The ◇ symbols denote values obtained from the variance method, and the □ symbols those derived from the nonoverlapping level formalism. Solid and double solid lines denote the microscopic calculations with Seeger-Perisho and Seeger-Howard levels, respectively, and the dashed and dot-dashed curves show the predictions of Gilbert and Cameron [20] and Rohr [19], respectively.

[6]. These authors assumed that the average gamma was defined by the expression

$$\Gamma_1 = \sum_J P_J \Gamma_J \ ,$$

where P_J gives the probability that the compound nucleus is formed with spin J. It has been more common in the past to average lifetimes rather than widths [18], in which case

$$\frac{1}{\Gamma_2} = \sum_J P_J / \Gamma_J \ .$$

In fact, if one constructs an autocorrelation function from equal contributions of functions with two or three different widths, the best fit gamma is actually between the values Γ_1 and Γ_2, although the difference between Γ_1 and Γ_2 is normally less than 25%, making this distinction less important. We have calculated the level density using both Γ_1 and Γ_2 and have averaged these to give the value denoted by level density from gamma.

A far more important question is that of level densities in the residual nucleus. As can be seen from the formulas for $\omega(E)$, the level density in the compound nucleus varies *linearly* with the sum of the transmission coefficients over all outgoing channels. For the lowest energies, the Hauser-Feshbach calculation depends only on known levels, while as the energy increases, the largest decay branches move to regions of the continuum. The present calculations include the lowest 20 levels in each final nucleus as individual levels, with the continuum formula used beyond this point.

Calculations were carried out with the tabulation of Rohr [19] and Gilbert and Cameron [20] and with pa-

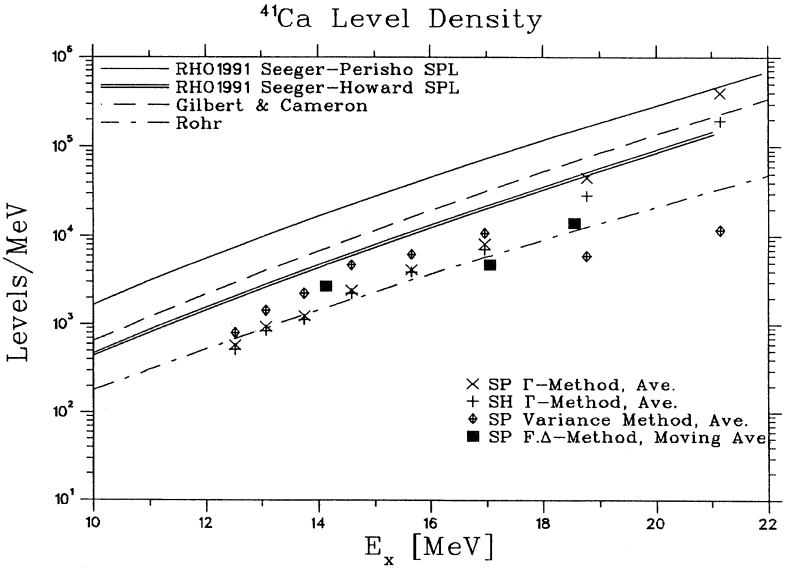

FIG. 5. Level density of ^{41}Ca inferred from fluctuation measurements compared with calculations and predictions. The × and + marks denote values derived from the gamma method with level densities in the final nuclei given by microscopic predictions based on Seeger-Perisho [15] and Seeger-Howard [16] single-particle states, respectively. The ◇ symbols denote values obtained from the variance method, and the □ symbols those derived from the nonoverlapping level formalism. Solid and double solid lines denote the microscopic calculations with Seeger-Perisho and Seeger-Howard levels, respectively, and the dashed and dot-dashed curves show the predictions of Gilbert and Cameron [20] and Rohr [19], respectively.

rameters obtained from statistical mechanical calculations [17] with the single-particle states proposed by Seeger and Perisho [15] and Seeger and Howard [16]. In general, the various predictions show a consistent shape, but differ somewhat in magnitude.

The general trend of the values obtained from the fluctuation analysis follows the slope predicted by the statistical mechanical calculation and by the compilations. A tendency for the experimental results to agree better with the Rohr and Seeger-Perisho tabulations is seen, with poorer agreement for the Seeger-Howard and Gilbert-Cameron tabulations. Note that the values deduced from the gamma technique are almost completely insensitive to the choice of level density parameters in the residual nuclei at the lowest energy (where only the tabulated level energies are used), but as the energy increases, they diverge. This is as expected, since the level density values in the compound nucleus for a given value of gamma show a linear dependence on the level densities in the residual nuclei. Thus, in this energy range, the level density results depend sensitively on the assumed final nucleus level densities with method 1. A substantial advantage to method 2 is that the residual level densities do not enter in the calculation. At the top energies, the uncertainty in the values of the level density deduced from method 1 increases substantially, while that for values from method 2 should remain roughly the same until the fluctuations become too small to measure reliably.

The fundamental requirement for Ericson theory to be valid is that the level width Γ be comparable to or greater than the level spacing D. Using the widths and spacing deduced from the Ericson analysis enables a check of this assumption. Γ varies slowly with J, but D varies rapidly with J, having a minimum for $J \approx 3$. The ratio Γ_J / D_J inferred from the Ericson analysis suggests that the fundamental assumption of Ericson theory is not met in the lowest 2–3 MeV of the excitation region studied.

Carlson and Barschall [4] have utilized a related procedure to obtain level density information at lower energies. In this limit it is assumed that interference between levels is small and that fluctuations are due to variations in the number of levels in an energy bin of given width as the energy varies or variation in the average neutron width of the levels. They show that if the cross section is averaged over a bin width Δ and the variance F of this averaged cross section relative to an average over an even larger averaging interval I is calculated, one obtains

$$F_I \Delta = (\pi \lambda^2) \frac{1}{\omega(E)} \sum_J \frac{g^2(J)(T_{n_l}^J)^2}{H(J)} (k_W + k_n) , \qquad (6)$$

where $g(J) = (2J+1)/(2I+1)(2i+1)$ and k_W and k_n are $\mathrm{Var}(\Gamma_n)/\langle \Gamma_n \rangle^2$ and $\mathrm{Var}(N)/\langle N \rangle$, respectively. They thus define the magnitude of the variances of the width and spacing distributions, since N is the number of levels in the energy bin. Under the usual assumptions [4], k_W is 2 and k_n is 0.27 at low energy, while the corresponding high-energy limits are 1 for both k_n and k_W. Thus the sum will be about 2 in both limits and this value was used in the present analysis.

An analysis procedure of the type performed by Carlson and Barschall [4] was performed on the present data. The bin widths Δ were determined so as to compensate for the increase in level density over the range; i.e., Δ over the range was varied as $1/\rho(E)$, where a first-order estimate of $\rho(E)$ was obtained from the parameters of Rohr [19]. Varying the value of Δ in the lowest bin scaled all other Δ values by the same factor. The appropriate value for the large averaging interval was chosen as in Ref. [4], by examining the magnitude of $F\Delta$ as a function of the large averaging interval I. This variation is large for small I, but eventually reaches a plateau; an I value corresponding to this region was used in the analysis.

Values obtained from this analysis are shown in Figs. 3–5 labeled "$F\Delta$ method." No systematic differences were found between the values extracted from this procedure and those deduced with the use of Ericson theory.

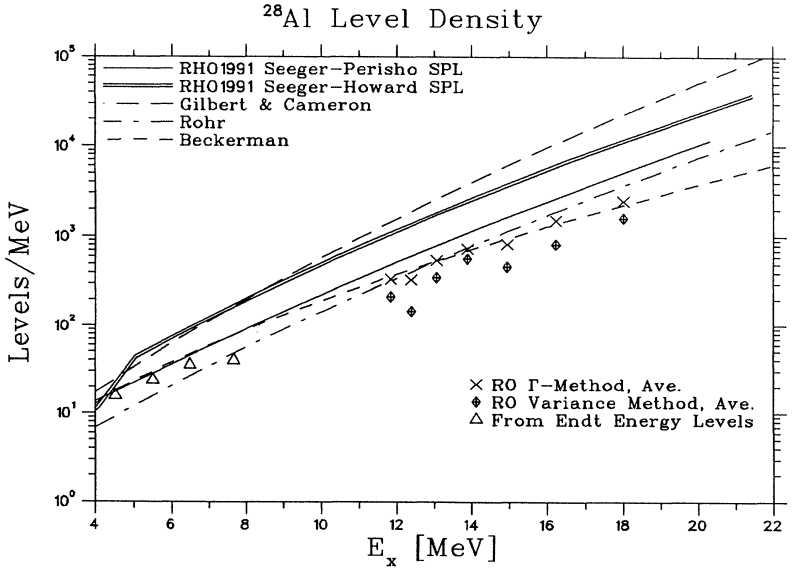

FIG. 6. Level density of ^{28}Al. Triangles denote values derived from Endt [21], while × and ◊ symbols denote results from the width and variance method, respectively, based on the level density of Rohr [19] in the residual nuclei. In addition to the predictions explained in Fig. 3, the prediction of Beckerman [22] is also shown.

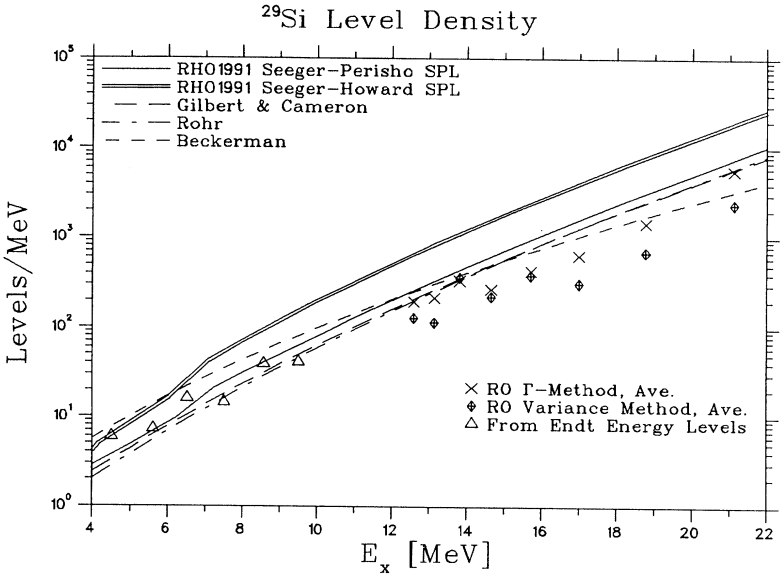

FIG. 7. Level density of ^{29}Si. Triangles denote values derived from Endt [21], while × and ◊ symbols denote results from the width and variance method, respectively, based on the level density of Rohr [19] in the residual nuclei. In addition to the predictions explained in Fig. 3, the prediction of Beckerman [22] is also shown.

These similarities are an obvious result of the very close relationship between Eqs. (3) and (6).

A broader test of the level density predictions can be made with the use of low-energy level density data. The levels listed in Endt [21] were summed to obtain values for the level density in the region below 6 MeV, and these results are shown in Figs. 6–8. Comparisons are presented with Gilbert and Cameron [20], Beckerman [22], and Rohr [19]. Of these compilations, the results of Rohr agree better than the other two, with a tendency to be above the data for all three compilations. The unorthodox level density form used by Beckerman may explain why the level density for his parameters has a somewhat different shape. Also shown are microscopic calculations based on the level schemes of Seeger and Perisho [15] and Seeger and Howard [16]. These are also somewhat too large. It is interesting to note that the Seeger-Perisho predictions are better for ^{28}Al and ^{29}Si, while the Seeger-Howard predictions are superior for ^{41}Ca.

A comparison of the present data was also made with the results of Ignatyuk, Smirenkin, and Tishin [23]. These authors propose that an energy-dependent a be used to deal with shell and collective effects. The form for a used is

$$a(E)=a_{\text{eff}}\left[1-\frac{\Delta}{E}(1-e^{-\gamma E})\right], \tag{7}$$

where γ is 0.05, a_{eff} is the asymptotic value of a at high energies, and Δ is the shell and pairing energy shift. The above form shows an increase of a with E if Δ is positive and a decrease of a with E if Δ is negative. Also, the same authors propose a dependence of a_{eff} on A of the form

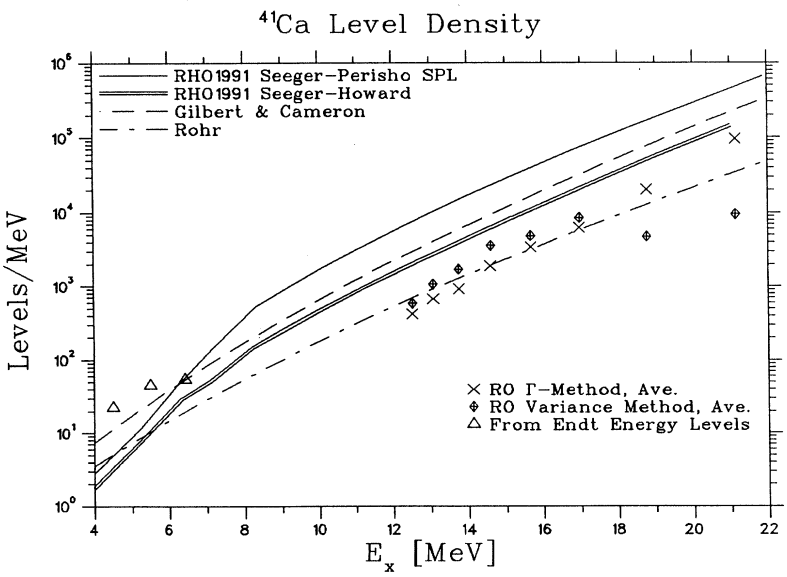

FIG. 8. Level density of ^{41}Ca. Triangles denote values derived from Endt [21], while × and ◊ symbols denote results from the width and variance method, respectively, based on the level density of Rohr [19] in the residual nuclei. In addition to the predictions explained in Fig. 3, the prediction of Beckerman [22] is also shown.

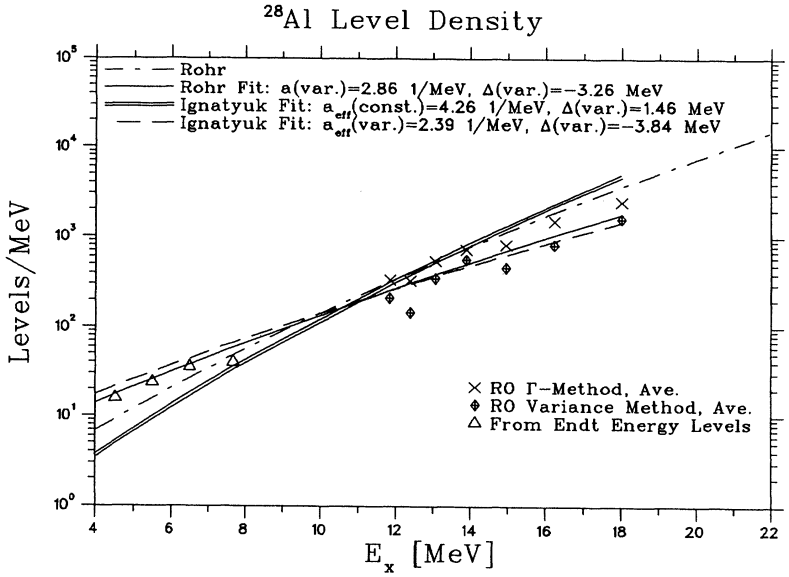

FIG. 9. Level density of ^{28}Al. Shown are the data points presented in Fig. 6 and the predictions of Rohr [19] (dot-dashed line) and a fit optimizing the representation of the data by varying a and the energy shift Δ (solid line). The double line shows a fit based on the formalism of Ignatyuk, Smirenkin, and Tishin [23] where Δ is varied and the dashed line a fit where both a_{eff} and Δ are varied.

$$a_{\text{eff}}/A=\alpha+\beta A \ . \tag{8}$$

Level densities for ^{28}Al, ^{29}Si, and ^{41}Ca derived from these values are compared with the present data in Figs. 9–11, where a_{eff} was determined from Eq. (8) and the Δ was varied to optimize the fit. As can be seen, the values of a_{eff} are too large, causing the best fit level density to have a steeper slope than the data.

A fit was also made by allowing both a_{eff} and Δ to vary. This gave results which were much better, and the a_{eff} values dropped by more than 30%. The results of Ignatyuk, Smirenkin, and Tishin included many heavier nuclei and appear to have too large a value for a_{eff} in this mass region.

A further search was conducted using a conventional (constant a) Fermi gas form. This fit is marked "Rohr fit," since the starting points for the parameters a and Δ were the values of Rohr. The fits of Ignatyuk, Smirenkin, and Tishin and Rohr produce similar quality representations of the data and are consistent roughly with $a=A/10$ and a back-shifted value for Δ (i.e., more negative than the usual 0 for odd-odd, Δ for even-odd or odd-even, and 2Δ for even-even nuclei).

A more recent paper by Ignatyuk, Istekov, and Smirenkin [24] has proposed alternative forms for a_{eff}. These include one in which a_{eff} is proportional to A and two forms in which a second term proportional to $A^{2/3}$ is also included. These produce predictions which are closer to the present results than those of Ref. [23], with the forms

$$a_{\text{eff}}=0.0792(A+A^{2/3})$$

and

$$a_{\text{eff}}=0.091A \ ,$$

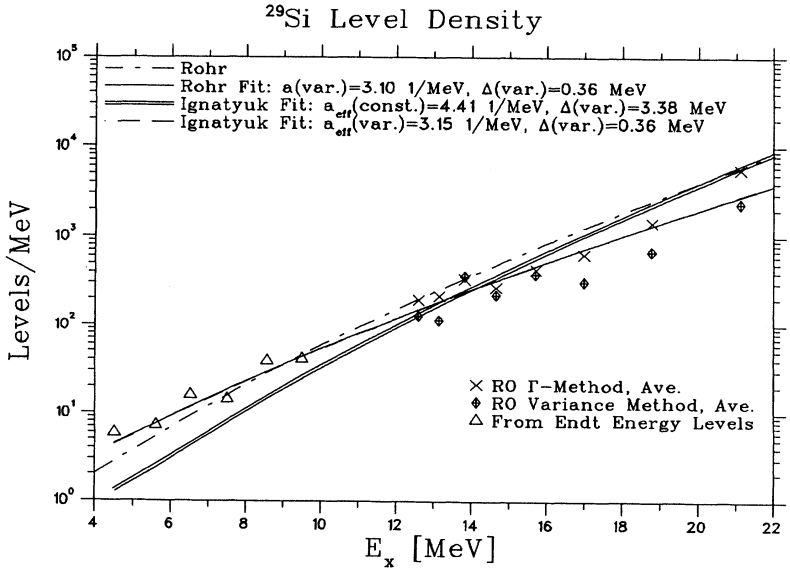

FIG. 10. Level density of ^{29}Si. Shown are the data points presented in Fig. 7 and the predictions of Rohr [19] (dot-dashed line) and a fit optimizing the representation of the data by varying a and the energy shift Δ (solid line). The double line shows a fit based on the formalism of Ignatyuk, Smirenkin, and Tishin [23] where Δ is varied and the dashed line a fit where both a_{eff} and Δ are varied.

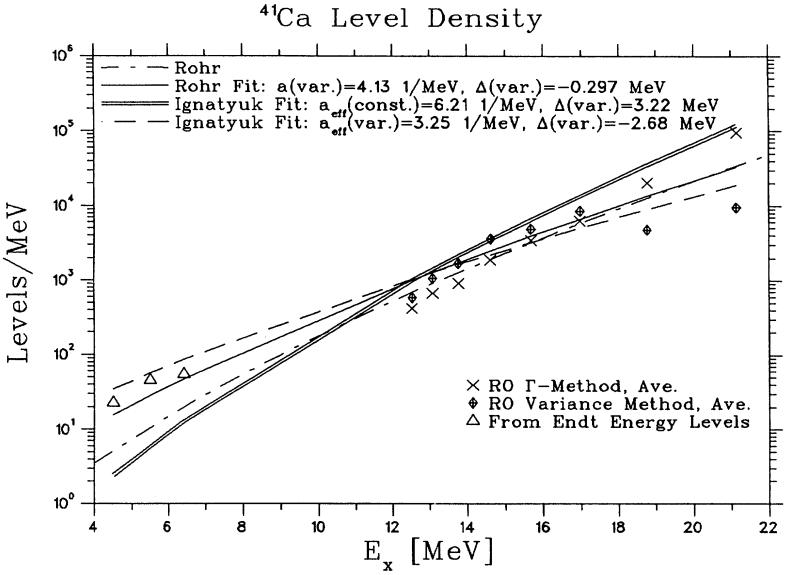

FIG. 11. Level density of ^{41}Ca. Shown are the data points presented in Fig. 8 and the predictions of Rohr [19] (dot-dashed line) and a fit optimizing the representation of the data by varying a and the energy shift Δ (solid line). The double line shows a fit based on the formalism of Ignatyuk, Smirenkin, and Tishin [23] where Δ is varied and the dashed line a fit where both a_{eff} and Δ are varied.

providing the best representation.

Further work on the topic of level densities deduced from fluctuations will require use of partial cross sections or lower neutron energies, if the region $A > 40$ is explored. The precision of these data is about 1%, but the fluctuations for the ^{40}Ca total cross section are already small enough for $E_n > 10$ MeV that the errors in level density are large. Presumably, an experiment which measured total cross sections between 1 and 6 MeV would have better prospects for obtaining level density information for $A > 40$ than one in the present energy range. Partial cross sections are harder to measure, but the fluctuations are much larger.

IV. SUMMARY

Measured values of the total neutron cross section for ^{27}Al, ^{28}Si, and ^{40}Ca have been subjected to an Ericson analysis. Two separate procedures have been used to deduce the level density. The most commonly used method is based on determining the average level width; this method has reasonable errors for low energies, but suffers in reliability as the excitation energy exceeds 15 MeV. Level density values can also be inferred from the variance of the cross section. These values are subject to similar errors as those from the width method at low energies, but do not show the same dramatic increase in errors as the energy increases. For ^{28}Al and ^{29}Si, the results from the Γ method are consistently higher than those from the variance method, while for ^{41}Ca, the low-energy region has the variance method results above the Γ method and the reverse situation at high energies. It appears that level densities may be obtained over a range of 8–12 MeV from total cross section measurements, but the errors are still approximately 40%. Nonetheless, such measurements reach an energy region which is difficult to study using other techniques and are particularly valuable. The present study clarifies the dependence of the Γ method on the level density parameters of the residual nuclei and finds somewhat better agreement between the two methods than was found previously. An obvious conclusion from this analysis is that fluctuation data on partial cross sections through the same compound nucleus would be helpful since these would not only provide additional level density values, but would also provide constraints on the residual level densities if the average cross sections are matched.

[1] T. Ericson, Phys. Rev. Lett. **5**, 430 (1960); Ann. Phys. (N.Y.) **23**, 340 (1963).
[2] M. G. Braga-Marcazzan and L. Milazzo-Colli, Prog. Nucl. Phys. **11**, 145 (1970); T. Ericson and T. Mayer-Kuckuk, Annu. Rev. Nucl. Sci. **16**, 183 (1968).
[3] A. Richter, in *Nuclear Spectroscopy and Reactions,* edited by J. Cerny (Academic, New York, 1974), Pt. B, pp. 343–391.
[4] A. D. Carlson and H. H. Barschall, Phys. Rev. **158**, 1142 (1967).
[5] S. M. Grimes, Nucl. Phys. **A124**, 369 (1969).
[6] V. Mishra, N. Boukharouba, S. M. Grimes, K. Doctor, R. S. Pedroni, and R. C. Haight, Phys. Rev. C **44**, 2419 (1991).
[7] R. W. Finlay, G. Fink, W. Abfalterer, P. W. Lisowski, G. L. Morgan, and R. C. Haight, in *International Conference on Nuclear Data for Science and Technology,* Jülich, FRG, 1991, edited by S. M Qaim (Springer, Berlin, 1992), p. 720.
[8] R. W. Finlay, W. Abfalterer, G. Fink, E. Montei, T. Adami, P. W. Lisowski, G. L. Morgan, and R. C. Haight, Phys. Rev. C **47**, 237 (1993).
[9] M. S. Moore, Nucl. Instrum. Methods **169**, 245 (1980).
[10] O. D. Simpson *et al.*, Nucl. Instrum. Methods **30**, 293 (1964).
[11] D. M. Brink and R. O. Stephen, Phys. Lett. **5**, 72 (1963).
[12] J. Rapaport, V. Kulkarni, and R. W. Finlay, Nucl. Phys.

A330, 15 (1979).
[13] F. D. Becchetti, Jr. and G. W. Greenlees, Phys. Rev. **182**, 1190 (1969).
[14] L. McFadden and G. R. Satchler, Nucl. Phys. **84**, 177 (1966).
[15] P. A. Seeger and R. C. Perisho, Los Alamos Report No. LA-3751, 1967 (unpublished).
[16] P. A. Seeger and W. M. Howard, Nucl. Phys. **A238**, 491 (1975).
[17] S. M. Grimes, J. D. Anderson, J. W. McClure, B. A. Pohl, and C. Wong, Phys. Rev. C **10**, 2373 (1974).
[18] P. Fessenden, W. R. Gibbs, and R. B. Leachman, Phys. Rev. Lett. **15**, 796 (1965).
[19] G. Rohr, Z. Phys. A **318**, 299 (1984).
[20] A. Gilbert and A. G. W. Cameron, Can. J. Phys. **43**, 1446 (1965).
[21] P. M. Endt, Nucl. Phys. **A521**, 1 (1990).
[22] M. Beckerman, Nucl. Phys. **A278**, 333 (1977).
[23] A. V. Ignatyuk, G. N. Smirenkin, and A. S. Tishin, Yad. Fiz. **21**, 485 (1975) [Sov. J. Nucl. Phys. **21**, 255 (1975)].
[24] A. V. Ignatyuk, K. K. Istekov, and G. N. Smirenkin, Yad. Fiz. **29**, 875 (1979) [Sov. J. Nucl. Phys. **29**, 450 (1979)].